
Article:

Panagi, M., Sommariva, Roberto, Fleming, Z. L. et al. (14 more authors) (2022) Daily evolution of VOCs in Beijing:chemistry, emissions, transport, and policy implications. Atmospheric Chemistry and Physics Discussions. pp. 1-29. ISSN: 1680-7367

https://doi.org/10.5194/acp-2022-379

---

https://doi.org/10.5194/acp-2022-379
Preprint. Discussion started: 27 June 2022

Daily evolution of VOCs in Beijing: chemistry, emissions, transport, and policy implications

Marios Panagi[1,2], Roberto Sommariva[1,3], Zoë L. Fleming[4], Paul S. Monks[1], Gongda Lu[3], Eloise A. Marais[5], , James R. Hopkins[6,7], Alastair C. Lewis[6,7], Qiang Zhang[8], James D. Lee[6], Freya A. Squires[7*], Lisa K. Whalley[9], Eloise J. Slater[10], Dwayne E. Heard[10], Robert Woodward-Massey[11], Chunxiang Ye[11], Joshua D. Vande Hey[2,12]

[1]Department of Chemistry, University of Leicester, Leicester, UK

[2]Department of Physics and Astronomy, Earth Observation Science Group, University of Leicester, Leicester, UK

[3]School of Geography, Earth and Environmental Sciences, University of Birmingham, Birmingham, UK

[4]Centre for Climate and Resilience Research (CR2), Department of Geophysics, University of Chile, Santiago, Chile

[5]Department of Geography, University College London, London, UK.

[6]National Centre for Atmospheric Science, University of York, UK

[7]Wolfson Atmospheric Chemistry Laboratories, University of York, UK

[8]Ministry of Education Key Laboratory for Earth System Modeling, Department of Earth System Science, Tsinghua University, Beijing, China

[9]National Centre for Atmospheric Science, School of Chemistry, University of Leeds, Leeds, UK

[10]School of Chemistry, University of Leeds, Leeds, UK

[11]Beijing Innovation Centre for Engineering Science and Advanced Technology, State Key Joint Laboratory for Environmental Simulation and Pollution Control, Centre for Environment and Health, College of Environmental Sciences and Engineering, Peking University, Beijing, China

[12]Centre for Environmental Health and Sustainability, University of Leicester, Leicester LE1 7RH, UK

*Now at British Antarctic Survey, Natural Environment Research Council, Cambridge CB3 0ET, UK

Correspondence to: Marios Panagi (mp670@le.ac.uk) and Joshua D. Vande Hey (jvh7@le.ac.uk)

Abstract. Volatile organic compounds (VOCs) are important precursors to the formation of ozone (O_3) and secondary organic aerosols (SOA) and can also have direct human health impacts. Generally, given the range and number of VOC species, their emissions are poorly characterised. The VOC levels in Beijing during two campaigns (APHH) were investigated using a dispersion model (NAME), and a chemical box model (AtChem2) in order to understand how chemistry and transport affect the VOC concentrations in Beijing. Emissions of VOCs in Beijing and contributions from outside Beijing were modelled using the NAME dispersion model combined with the emission inventories and were used to initialize the AtChem2 box model. The modelled concentrations of VOCs from the NAME-AtChem2 combination were then compared to the output of a chemical transport model (GEOS-Chem). The results from the emission inventories and the NAME air mass pathways suggest that industrial sources to the south of Beijing and within Beijing both in summer and winter are very important in controlling the

VOC levels in Beijing. A number of scenarios with different nitrogen oxides to ozone ratios (NO_x/O_3) and hydroxyl (OH) levels were simulated to determine the changes in VOC levels. In Beijing over 80% of VOC are emitted locally during winter, while during summer about 35% of VOC concentrations (greater for some individual species) are transported into Beijing from the surrounding regions. Most winter scenarios are in good agreement with daily GEOS-Chem simulations, with the best agreements seen for the modelled concentrations of ethanol, benzene and propane with correlation coefficients of 0.67, 0.63 and 0.64 respectively. Furthermore, the production of formaldehyde within 24 hours air travel from Beijing was investigated, and it was determined that 90% of formaldehyde in the winter and 83% in the summer in Beijing is secondary, produced from oxidation of non-methane volatile organic compounds (NMVOCs). The benzene/CO and toluene/CO ratios during the campaign is very similar to the ratio derived from literature for 2014 in Beijing, however more data are needed to enable investigation of more species over longer timeframes to determine whether this ratio can be applied to predicting VOCs in Beijing. The results suggest that VOC concentrations in Beijing are driven predominantly by sources within Beijing and by local atmospheric chemistry during the winter, and by a combination of transport and chemistry during the summer. Moreover, the relationship of the NO_x/VOC and O_3 during winter and summer shows the need for season-specific policy measures.

https://doi.org/10.5194/acp-2022-379
Preprint. Discussion started: 27 June 2022

1 Introduction

Volatile organic compounds (VOCs) are reactive chemicals emitted from a variety of anthropogenic sources such as vehicles, industry and solvents, as well as from biogenic sources. VOCs are important precursors to the formation of secondary pollutants, and can form pollutants such as secondary organic aerosol (SOA) and ozone (O_3) through photochemical reactions with nitrogen oxides (NO_x, ($NO_x \equiv NO + NO_2$)) (Carter and Seinfeld, 2012; Atkinson, 2000, Monks et al., 2009; Monks et al., 2015). Exposure to O_3 pollution can lead to adverse health effects such as lung inflammation and airway hyperactivity (Uysal and Schapira, 2003; Liu et al., 2018). The production of O_3 under high NO_x conditions is limited by the availability and reactivity of VOCs (VOC-limited), while under low NO_x conditions it is limited by the availability of NO_x (NO_x-limited) (Sillman 1999). The VOC/NO_x ratio is therefore very important in order to understand the ozone formation potential and develop policies to reduce O_3 concentrations (LaFranchi et al., 2011). Additionally, human exposure to some VOCs at elevated ambient levels has been associated to adverse health outcomes. Formaldehyde is known to induce acute poisoning and is a probable carcinogen, while benzene and other traffic related VOCs could cause respiratory effects by irritating the airways (Rumchev et al., 2007; Tang et al., 2009).

Previous work has shown that during winter, biofuel and coal burning are significant sources of VOCs in Beijing (Liu et al., 2016; Z. Zhang et al., 2016). For example, Gu et al. (2019) studied the presence of 99 non-methane VOCs (NMVOCs) in Beijing during winter and summer. They found that the concentrations of total NMVOCs decreased most in winter polluted days, then in summer polluted days, in summer normal (i.e. less polluted) days, and least in winter normal days and that the oxygenated volatile organic compounds (OVOC) decreased most in summer polluted days, then in summer normal days, in winter polluted days and least in winter normal days.

Yao et al. (2015) determined from studying 18 different sized diesel trucks that carbonyls, aromatics and alkanes were the dominant species emitted, with carbonyls accounting for 43-69% of the total VOCs emitted. Yang et al., (2018a), determined that VOC levels decreased approximately 50% during an enhanced emission control period, where all emission sectors were controlled except for the residential sector. Furthermore, they observed that during the study period, all observed high VOC episodes in Beijing occurred during southerly winds indicating the effect of the meteorology and the influence of the heavily industrialised regions to the south of the city.

In megacities where motor vehicles can be the dominant sources of air pollution, the VOCs and carbon monoxide (CO) emissions are highly correlated due to co-emissions and therefore, by using the VOC/CO enhancement ratios, it is possible to predict the VOC levels and speciation (Parrish et al., 2009; Warneke et al., 2012). Similarly, von Schneidemesser et al. (2010) determined that there were similar reductions in both CO and VOCs in London correlated during the period 1998 to 2007 and for the majority of species the VOC/CO ratios remained steady over the study period.

A number of modelling studies have looked into policy controls to reduce ozone. Using the GEOS-Chem chemical transport model (CTM) it has been postulated that the $PM_{2.5}$ decrease in China results in increases in O_3 owing to the slowing down of reactive uptake in HO_2 and NO_x from aerosols and the need for VOC controls to reduce ozone and offset the effect of the $PM_{2.5}$

decrease (Wang et al., 2013, Li et al., 2019a, Li et al., 2019b). The emission inventories that are used in chemical transport models are vital for informing policies, but there are many discrepancies among different emission inventories such as underestimations of VOCs and emerging sources for oxygenated VOCs (OVOCs) (Saikawa et al., 2017, Karl et al., 2018, McDonald et al., 2018).

The objective of this study is to determine what controls VOC levels in Beijing, the effects on VOC levels under different scenarios and how they affect ozone formation potential. Furthermore, the relationship of the NO_x/VOC of the measured VOCs and the modelled VOCs is investigated. Approaches used include: analysis of VOC/CO ratios, using the NAME dispersion model to investigate air mass pathways and transportation of VOCs, using NAME coupled with the AtChem2 box model to investigate how chemistry can affect VOC levels, and use of a CTM (GEOS-Chem). Only emissions that are within the 1 day backward footprints were considered, in order to focus on the immediate contributions from within Beijing and nearby regions outside of Beijing.

2 Methods

2.1 In situ measurements

VOCs were measured during the two Air Pollution and Human Health (APHH) campaigns (Shi et al., 2019) at the Institute of Atmospheric Physics (IAP) tower (39.975°, 116.377°), located in the city centre of Beijing between two very busy ring roads. VOCs were measured using a dual-channel gas chromatography with flame ionization detector (DC-GC-FID) (Hopkins et al., 2011) instrument, which is comprised of two GC instruments, and formaldehyde, HCHO, was measured by laser-induced fluorescence spectroscopy (LIF) (Cryer et al., 2016; Slater et al., 2020; Whalley et al., 2021). CO measurements at the IAP site were made using six clustered electrochemical sensors (Alphasense Ltd.) encased in a 2 × 3 formation. OH was measured using the Fluorescence Assay by Gas Expansion (FAGE) instrument. O_3, NO and NO_2 were measured with the commercial instruments TEI 49i, TEI 42i and Teledyne CAPS, respectively (Shi et al., 2019). Measurements from the "winter" campaign (10th of November 2016 to the 31st of November 2016) and the "summer" campaign (26th of May 2017 to the 24th of June 2017) are compared with the modelling results from this study.

2.2 The NAME dispersion model

The air mass pathways arriving at Beijing during the study period were modelled using the Numerical Atmospheric Modelling Environment (NAME) model created by the Met Office UK (Jones et al., 2007). NAME uses meteorological fields from the Unified Model (Brown et al., 2012), to track the pathways of hypothetical inert tracers. These fields during our study period have a resolution of 0.23° longitude by 0.16° latitude with 59 vertical levels up to an approximate height of 30 km. For this study, 3-hourly footprints are modelled by 1 day backwards runs with a resolution of 0.25° x 0.25° of all air masses in a layer from 0 – 100 m above ground from 10th of November 2016 to 30th of November 2016 and 26 of May 2017 to 24th of June 2017 (see Fig. 1). The units are based on a release of a known quantity of air masses (hypothetical particles) in grams (g) during an integrated time-period (s) and the results are displayed per grid box, which has a volume component.

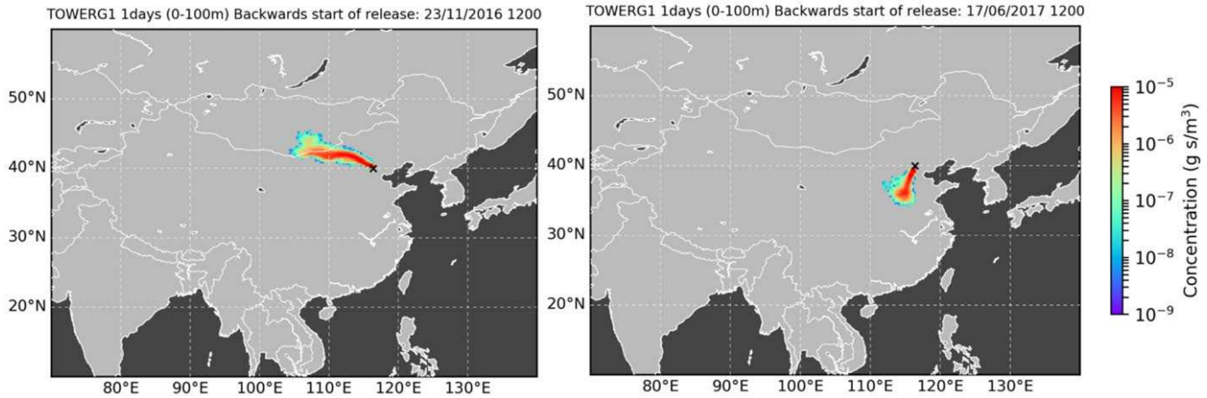

Figure 1: Example of a 24 hour backwards NAME footprint arriving at the IAP meteorological tower during the winter campaign (left) and the summer campaign (right)

The modelled NAME footprints are combined with gas emission inventories to calculate the mixing ratio of the species at the measurement site (Oram et al., 2017, Panagi et al., 2020). The VOC concentrations were calculated by deriving the sensitivities of the NAME air masses (units [g m^{-3}] / [g m^{-2} s^{-1}], i.e. s m^{-1}) which are then multiplied by the VOC fluxes from the emission inventories (dimensionally, s m^{-1} × Kg m^{-2} s^{-1} = Kg m^{-3}) to get the concentration affecting Beijing from each grid box. The mass concentrations are then summed and converted to mixing ratios by dividing them by the molar mass, dividing again by the air density and multiplying by 1×10^9 to convert to ppbV. For each species, only the emissions occurring within the timescale of the NAME footprint are considered.

In this study, the 2016 and 2017 monthly Multi-resolution Emission Inventory for China (MEIC, Li et al., 2017) and the 2014 Community Emissions Data Systems (CEDS, Hoesly et al., 2018) emission inventories were used to calculate the pollution transported to Beijing from surrounding regions. From MEIC the inventories of CO, benzene, toluene, ethane, propane, acetone and formaldehyde were used, and from CEDS the ethylene, acetylene and ethanol emission inventories were used, as these species are not part of MEIC. For both the emission inventories, the resolution used was 0.25° x 0.25° to match the resolution of the NAME outputs. For this work, the contributions of VOCs to Beijing were modelled to arise from two regions, Beijing (any sources emitted within Beijing) and any sources within the 1 day air mass footprint outside of Beijing (sources emitted and transported from outside of Beijing to Beijing.

2.3 The AtChem2 atmospheric chemistry box model

AtChem2 (Sommariva et al., 2020) is a box model for atmospheric chemistry designed to use the Master Chemical Mechanism (MCM, http://mcm.york.ac.uk/, last accessed: 22 September 2020) which describes the gas-phase oxidation of 143 (in version 3.3.1) primary emitted VOCs. AtChem2 can be used to calculate a wide variety of chemical and physical variables including photolysis rates, reaction rates, chemical species concentrations, sun declination, solar zenith angle. In this study, since there is no chemistry involved in the mixing ratios modelled from the combination of NAME footprints with the emission inventories, the AtChem2 box model was used to estimate the impacts of chemical processes on the emitted VOCs.

https://doi.org/10.5194/acp-2022-379
Preprint. Discussion started: 27 June 2022

A subset of the MCM was used, including only inorganic reactions, methane (CH_4) reactions and the reactions of the VOCs being investigated (benzene, toluene, ethane, propane, ethene, acetylene, acetone, formaldehyde and ethanol). The MCM subset includes 4106 reactions and 1356 species. In order to assess the effect of chemical oxidation on the modelled and observed VOC concentrations, the mixing ratios derived from the combination of NAME footprints with the emission inventories were used to initialise the model. Moreover, O_3, NO_2, NO, CO and OH measurements made at the IAP site during the APHH campaign (Shi et al., 2019) were used as constraints in the model for each 3 hourly 1 day backward footprint. The modified concentrations with chemistry were calculated for the same timescale as each footprint is starting and ending (24 hour reactions only). This novel approach of coupling NAME with a box model allows us to distinguish and understand both the meteorological and chemical factors that drive VOC concentrations in Beijing, as illustrated in Figure 2.

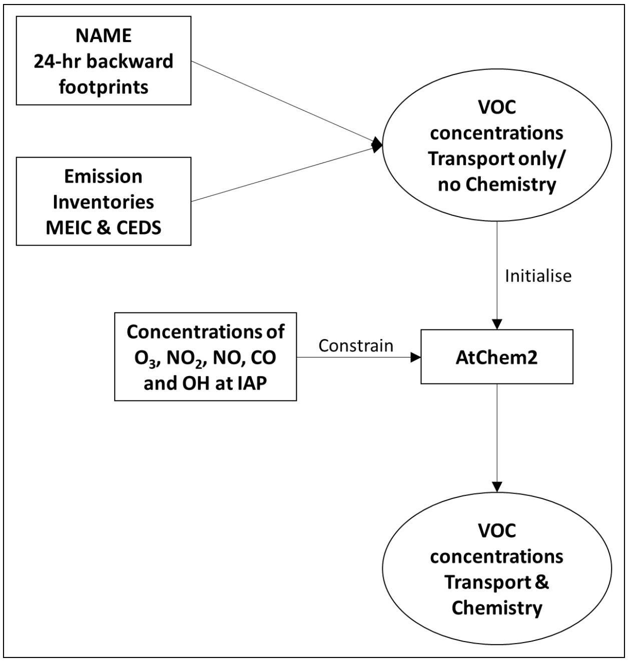

Figure 2: AtChem2 combined with NAME dispersion footprints (NAME-AtChem2).

2.4 The GEOS-Chem chemical transport model

To put the outputs of this novel modelling approach into a regional context, a chemical transport model (CTM) was utilised for the winter case. CTMs are typically run at coarser spatial resolutions than dispersion models, but integrate meteorology with gas- and aerosol-phase chemistry, which can provide better understanding on the limitations presented from the combination of NAME-AtChem2. Surface VOC concentrations over China coincident with the APHH campaign in November 2016 were simulated using the GEOS-Chem CTM version 12.0.0 (https://doi.org/10.5281/zenodo.1343547) nested over East Asia (-11-55°N, 60-150°E) at 0.5° × 0.625° (latitude × longitude), as described by Lu et al. (2021). The model includes detailed tropospheric HO_x-NO_x-VOC-ozone-aerosol chemistry. Anthropogenic emissions for China are from the national MEIC inventory (Li et al., 2017; Zheng et al., 2018). Other regionally relevant emissions in the model include biomass burning (Giglio et al., 2013), biogenic VOCs (Guenther et al. 2012), and soil NO_x (Hudman et al., 2012). The model is spun-up for 2 months before sampling daily 24-hour mean surface concentrations of seven VOCs (benzene, toluene, ethane, propane, acetone, formaldehyde and ethanol) in November 2016 for comparison to NAME-AtChem2 outputs averaged over the GEOS-Chem grid square coincident with the APHH sampling site.

3 Results and Discussion

3.1 VOC:CO ratios

Studies have suggested that the ratio between VOC and CO does not differ much from year to year and, therefore, that it can be used as a reliable predictor of the VOC levels. For example, in London the VOC/CO ratio for the majority of the VOC species did not change significantly during the 10 years from 1998 to 2007 (von Schneidemesser et al., 2010). Using this hypothesis, the average measured VOC/CO ratio for benzene and toluene in Beijing was calculated. Moreover, an average VOC/CO ratio was derived using VOC data from the literature (Li et al., 2015) and CO data during the time of the measurements reported in the literature from a nearby network station in Beijing (Shi et al., 2019) between 13 of November to 22 of November 2014 and compared to the same period in 2016. The derived ratios are very similar between the two years, with benzene/CO ratios of 0.92 and 1.06 and toluene/CO ratios of 1.13 and 1.10 in 2014 and 2016, respectively. These derived ratios were multiplied by the measured CO (from APHH) in 2016 to investigate whether they could be used to predict VOC levels and daily variations. In addition, the measured ratios from November 2016 are multiplied by the CO modelled using NAME and emission inventories (Panagi et al., 2020) to provide an additional comparison.

As shown in Figure 3, during the winter campaign the measured VOC/CO ratio capture the VOC concentrations and variations well. Using the ratio for each year, the correlation coefficients of benzene measurements from the campaign with the measured benzene/CO ratio from 2014 and 2016 are $r = 0.98$ and for the toluene measurements are $r = 0.91$ with the measured toluene/CO ratio from 2014 and 2016. Furthermore, the correlation coefficients from the measured VOC/modelled CO are $r = 0.83$ for benzene and $r = 0.82$ for toluene. The VOC/CO ratio technique can be helpful in understanding the VOC levels in situations where there are no available measurements, although long term and more detailed VOC measurements in Beijing would be ideal to investigate this further. Furthermore, a decent estimate of VOC levels for this period in Beijing can be obtained by using the CO modelled using the NAME footprints and the emission inventories with a VOC/CO ratio to provide information on the VOC concentrations if data is not available.

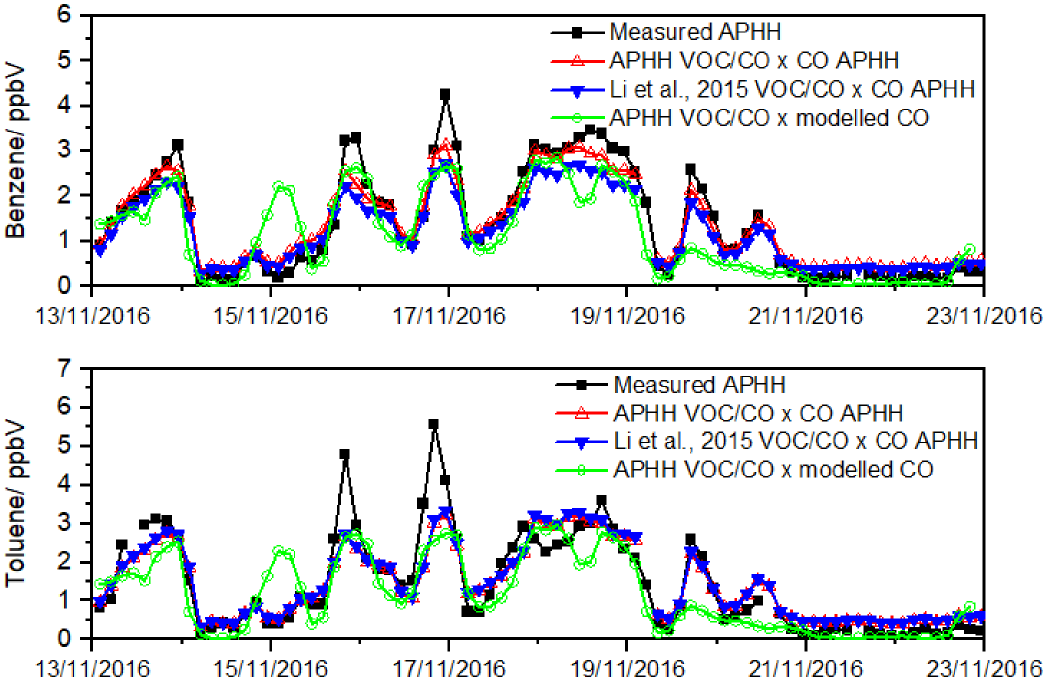

Figure 3: the relationship between VOCs measured during the winter APHH campaign, calculated from the measured VOC/CO ratio during 2016 and 2014 and calculated using the modelled NAME CO during the winter campaign. 190

3.2 Modelling air masses, the emissions of VOCs and sectoral contributions to Beijing

The pathways of the air masses and the regions the air masses passed over are important to understand how the air masses are influenced by the pollution emissions from those regions, as well as how the pollution is transported (Donnelly et al., 195 2016). Some regions are more polluted than others, which can lead to more pollution being transported to Beijing from those regions (Li et al., 2019c). To investigate the pathways of air masses arriving at Beijing modelled with NAME, the domain was separated into four quadrants (North-West (N-W), North-East (N-E), South-West (S-W) and South-East (S-E), see Figure 4). The four quadrants intersect at the Institute of Atmospheric Physics (IAP) meteorological tower where the measurements for the APHH campaign took place.

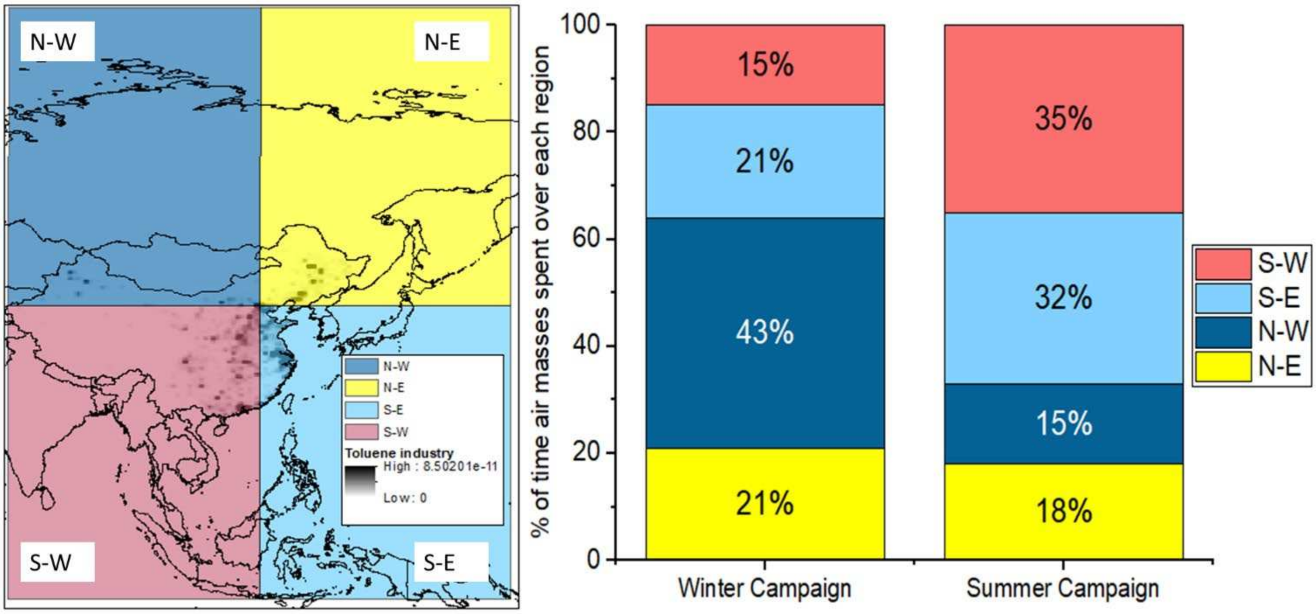

Figure 4: The four quadrants used to investigate the air mass pathways distribution, together with the Industrial toluene emissions (kg m^2 s^{-1}) from MEIC (left),). Percentage of air mass pathways distribution over the four quadrants during the two campaigns (right).

As observed in Figure 4, the air mass distributions for the winter and summer campaigns differ considerably. During the winter campaign, the air masses spent more time over the regions north of Beijing (64%) and during the summer campaign the air masses spent more time south of Beijing. (67%). A considerably higher density of anthropogenic sources is located in the regions south of Beijing: as an example, Figure 4 shows that the emissions of toluene from industrial sources are largely concentrated in the SW and SE quadrants. It is therefore important to study the air masses arriving at Beijing from the south, as these can affect the pollution transported to Beijing, which reveals the importance and need for stricter control measures in different areas in different seasons (Panagi et al., 2020).

Using the NAME footprints combined with the VOC emission inventories, it is possible to model the sectoral contributions and transportation of VOCs from different source regions to Beijing. Figure 5 shows the sectoral and spatial contributions from sources emitted within Beijing and sources emitted and transported from outside Beijing within the 1 day air mass travel. This enables local contributions to be distinguished from regional contributions, by sector, during the winter and summer campaigns.

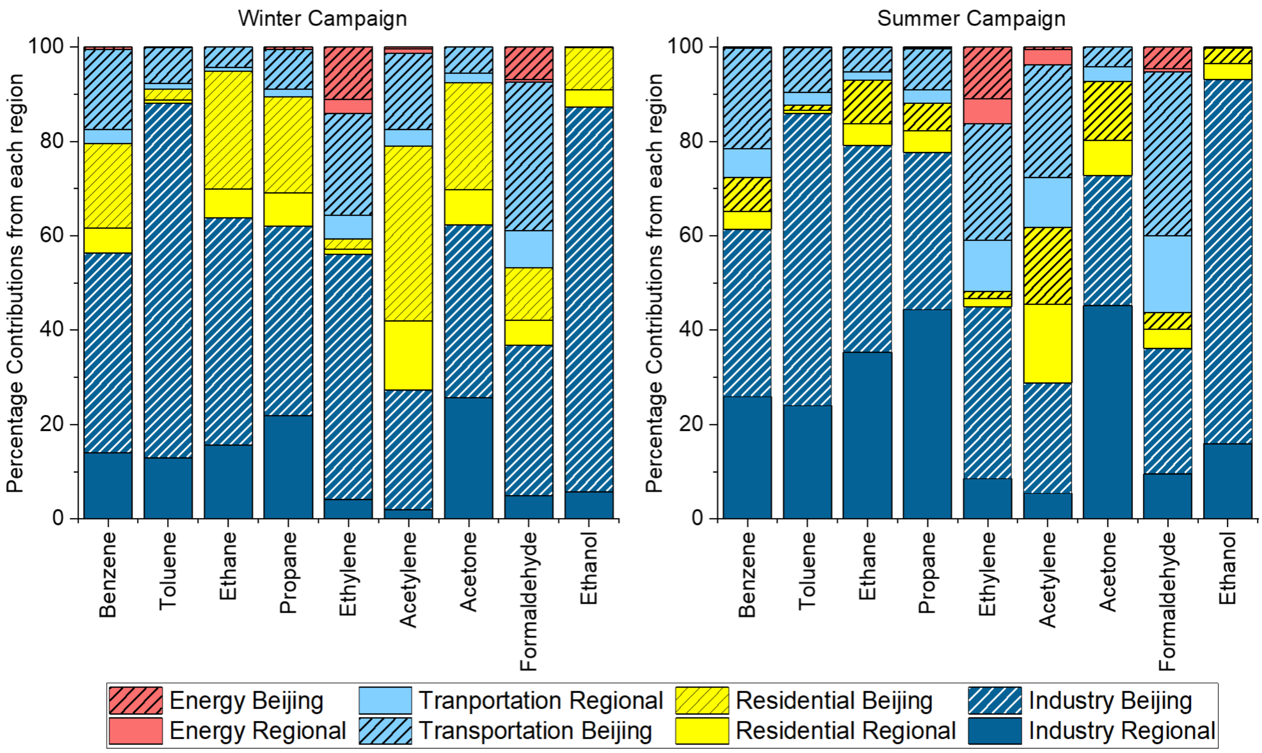

Figure 5: VOC contributions (in percentage) from each emission sector during the winter and summer campaign from Beijing and the surrounding region

220 During winter, approximately 80% of the VOCs affecting the levels in Beijing are emitted from local sources (i.e., within the city) and the rest from sources outside of Beijing within the 24 hour air mass travel period. The largest contributors from outside Beijing during the winter campaign were the industrial emissions of acetone, propane, ethane, toluene and benzene, and residential regional emissions of acetylene. During the summer campaign, an increase in the VOCs affecting Beijing that originates from outside of Beijing was observed within one day of travel, with approximately 35% of the VOC concentrations transported to Beijing from regions outside of the city compared to the 20% that was observed in the winter. The increase in the regional contributions during the summer is due to the air masses spending more time over the regions south of Beijing, where most of the emissions originate (see Figure 4), compared to the winter months where the air masses spend more time in the North and Northwest. During the one day runs, the contributions to Beijing from propane and acetone are highest from outside of Beijing. The results from the emission inventories and the air mass pathways suggest that industrial sources to the south of Beijing and within Beijing are very important drivers of the VOC levels in Beijing both in summer and winter.

Table 1: Average concentrations of measured and modelled VOCs (ppbV) from a series of scenarios to assess the impact of chemical processing on modelled VOCs, and the O_3, NO_x and OH concentrations constrained in the model runs

VOC	Measured[a]	NAME[b]	S1[c]	S2[d]	S3[e]	S4[f]	S5[g]
WINTER							
Benzene	1.5	2.1	2.1	2.0	2.0	2.0	1.7
Toluene	1.7	7.8	7.1	6.8	6.1	5.7	2.9
Ethane	8.6	3.4	3.4	3.4	3.4	3.4	3.2
Propane	6.0	3.7	3.6	3.6	3.5	3.4	3.0
Ethylene	6.9	5.1	4.4	4.1	3.6	3.2	1.3
Acetylene	5.3	2.0	2.0	2.0	1.9	1.9	1.7
Ethanol	11.7	6.5	6.1	5.9	5.6	5.3	3.6
Acetone	7.2	0.6	1.0	1.2	1.6	1.8	3.9
Formaldehyde	1.9	0.8	7.9	10.2	15.9	18.6	27.4
O_3 /ppbV		-	8.9	17.8	8.9	17.8	8.8
NO_x /ppbV		-	71.9	72.0	36.0	36.0	72.6
OH /molecule cm^{-3}		-	1.4E+05	2.0E+05	4.1E+05	5.2E+05	2.3E+06
SUMMER							
Benzene	0.5	1.3	1.1	1.0	1.1	1.0	0.9
Toluene	1.0	4.9	2.2	1.6	1.8	1.2	0.9
Ethane	3.5	1.8	1.8	1.8	1.7	1.7	1.7
Propane	4.4	2.3	2.0	1.8	1.9	1.7	1.6
Ethylene	1.3	2.6	0.8	0.4	0.5	0.3	0.3
Acetylene	1.2	0.8	0.7	0.6	0.7	0.6	0.6
Ethanol	5.5	3.1	1.9	1.6	1.7	1.4	1.3
Acetone	3.6	0.5	2.2	2.8	2.6	3.2	3.7
Formaldehyde	4.3	0.4	12.3	13.3	12.2	12.6	11.0
O_3 /ppbV		**-**	55.8	111.7	55.8	111.6	55.8
NO_x /ppbV		**-**	25.5	25.4	12.7	12.7	25.5
OH /molecule cm^{-3}		**-**	1.6E+06	2.6E+06	2.6E+06	4.0E+06	3.7E+06

[a] Mean campaign VOC average

[b] Modelled values from the combination of MEIC and NAME

[c] S1: Constraining original measurements (O_3, NO_2, NO, CO measured at the IAP tower) in NAME-AtChem2 runs

[d] S2: Constraining original measurements and doubling O_3 in NAME-AtChem2 runs

[e] S3: Constraining original measurements and halving NO_2 and NO in NAME-AtChem2 runs

[f] S4: Constraining original measurements and doubling O_3 and halving NO_2 and NO in NAME-AtChem2 runs

[g] S5: Constraining OH measurements only in NAME-AtChem2 runs

3.3 How VOC levels are affected by chemical evolution

The results obtained using NAME together with the emission inventories are based on the assumptions of no impact of oxidative chemistry during the 24h travel of an air mass. In order to investigate the effect of the chemistry, the Atchem2 box-model was initialized with the VOC concentrations modelled by coupling NAME with the emission inventories (see section 2.3). The model assumes NO_x and O_3 (and therefore OH) are homogeneous along the entire trajectory, which does not necessarily reflect reality and for this reason, the model was run under five different scenarios as outlined below. The five scenarios are used to investigate how the assumptions on the chemistry affects the VOC concentration during the 24-h transport pathways. The scenarios during the campaigns are:

- S1: Constrained to measurements of O_3, NO_2, NO, CO at the IAP tower. This is the base scenario and assumes that O_3, NO_x and CO are the same along the trajectory as in Beijing.
- S2: Constrained to measurements of NO_2, NO, CO and to double the O_3 measured at the IAP tower – to observe how higher ozone levels along the trajectory affects the chemistry.
- S3: Constrained to measurements of O_3, CO and half the NO_2 and NO measured at the IAP tower – to observe how NO_x limitation affects the chemistry.
- S4: Constrained to measurements of CO, double the O_3 and half the NO_2 and NO measured at the IAP tower – to observe how the NO_x/O_3 ratio affects the reactive chemistry with the VOCs.
- S5: Constrained to OH measurements only – to account for any underestimation of OH in the previous scenarios compared to the measured OH at IAP.

The results of the different simulation scenarios were compared against the measurements of each VOC at the IAP tower in Beijing during the two campaigns. The mean measured and modelled concentrations for the VOC species are shown in Table 1. The majority of the VOC emissions are underestimated in the emission inventories, except the toluene concentrations that are overestimated (Acton et al., 2020). The measured and modelled datasets are normalised by their mean (campaign average) just for ease of visualisation and to remove the bias caused by the overestimations/underestimations of the emissions, and presented in Fig. 6. It is observed that during the winter APHH campaign, the modelled concentrations calculated with NAME + emission inventories, and the ones calculated with the AtChem2 chemical box model are well correlated, as discussed below, and therefore this approach can be considered able to predict observed VOC variability.

The correlation coefficients of the measured vs modelled VOC species can be used to quantify how well the trajectories are able to capture the emissions affecting Beijing and whether there is any impact from the chemistry. During the winter campaign the correlation coefficients of the measured vs the modelled VOCs with no chemistry involved (i.e. calculated using just NAME with the emission inventories), show a good agreement for all species with correlation coefficients in the range of r = 0.82 – 0.89, with only ethanol showing the lowest correlation (r = 0.76). When chemistry was introduced into the box model, the correlation coefficients increased slightly for all species in the range of r = 0.84 – 0.91 for the scenarios S1 – S4, except acetone and formaldehyde. In scenario S5, where OH is at high levels (OH measured at Beijing), the correlation coefficients decreased to r =0.4 – 0. 88. The decrease in the correlation during the higher OH scenario was due to the faster loss of the VOCs by reacting with OH. The highest correlation decrease was observed for toluene and ethene, which are the most reactive species out of the hydrocarbons investigated. On the other hand, the correlation coefficient of acetone and formaldehyde when the chemistry is introduced decreases to r = 0.45 and r = 0.32 respectively and increases as the OH reaches higher levels to r = 0.80 and r = 0.87 respectively. The changes in the VOC correlation coefficients are indicating how the species are affected by loss and formation of secondary products from the oxidation of the VOCs in Beijing.

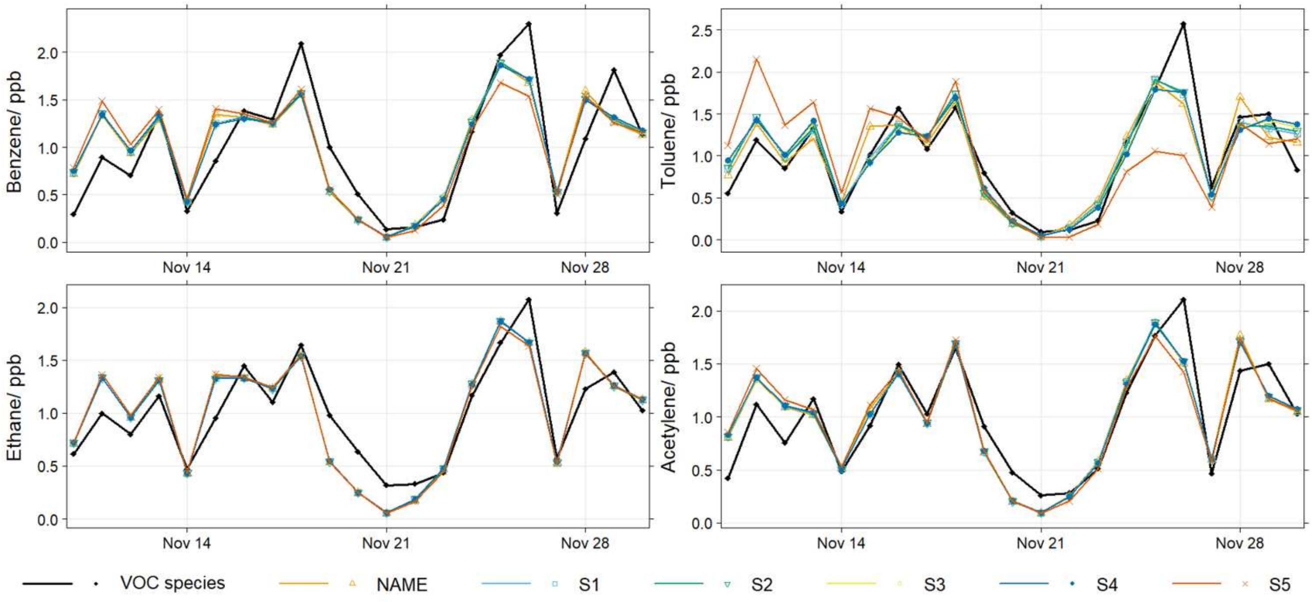

Figure 6: Normalised plots from the five modelled scenarios vs measured VOC concentrations during the winter campaign (scenarios are detailed in Table 1)

During the winter, scenario S5 (where OH was constrained to the measurements and not calculated from the model and was therefore higher), leads to higher loss of hydrocarbon species with the smallest effects for ethane and benzene of approximately 5% and 20%, respectively, and the highest effect for toluene and ethene of approximately 63% and 75%, respectively. In this scenario, for the photochemically produced OVOCs such as formaldehyde and acetone an increase in production of approximately 550% and 3500%, respectively, is observed when OH is higher. Comparing scenarios S2 and S3 one can observe that even though the NO_X/O_3 ratio is the same, the lower concentrations of both pollutants in S3 results in higher OH, which causes greater loss of hydrocarbons and higher production of OVOCs than when there are higher concentrations of NO_X and O_3. When the two scenarios are combined in scenario S4, OH increases more and higher loss of hydrocarbons and production of OVOCs is observed.

During the summer campaign, the correlations of the normalised modelled and measured VOCs are not in good agreement. The highest correlation coefficient is observed for acetylene with a range of 0.41 to 0.53. The poor correlation between the measured and modelled VOCs during the summer could be because of a variety of reasons such as, missing sources from the emission inventories and uncertainties in the dispersion of the NAME footprints. Furthermore, during the summer, the reactivity of the VOC species is higher owing to higher OH levels, which decrease the lifetimes of VOC species and change the composition of the air masses before they arrive at Beijing, with higher uncertainties when modelling species arriving from further away. As observed from the NAME distribution of the air masses during the summer, an increase in the emissions that originate from outside of Beijing is seen compared to the winter where the majority of the emissions are local and the chemistry tests can be more realistic for the local region/smaller footprint.

In the summer (Fig. 7), the OVOCs do not follow the same relationship compared to the winter campaign or with each other. The higher production of formaldehyde is taking place when O_3 is doubled in scenario S2 with an increase of approx. 3000 % within 24 hours, while the highest production in acetone is taking place during S5 when OH measured is constrained with 634 % increase. Moreover, the relationship between scenarios S2 and S3 in the summer does not follow the same relationship as in the winter. While the OH concentrations simulated from both scenarios are similar and the NO_x/O_3 ratio are the same, the higher destruction of the species is observed in the S2 scenario where both NO_x and O_3 are at higher levels. All species showed a higher destruction (hydrocarbons) and production (formaldehyde, acetone) during scenario S2 compared to scenario S3 except for ethane. This shows the importance of understanding how the VOCs are affected by pollution related chemistry along their pathway and not just at an individual point.

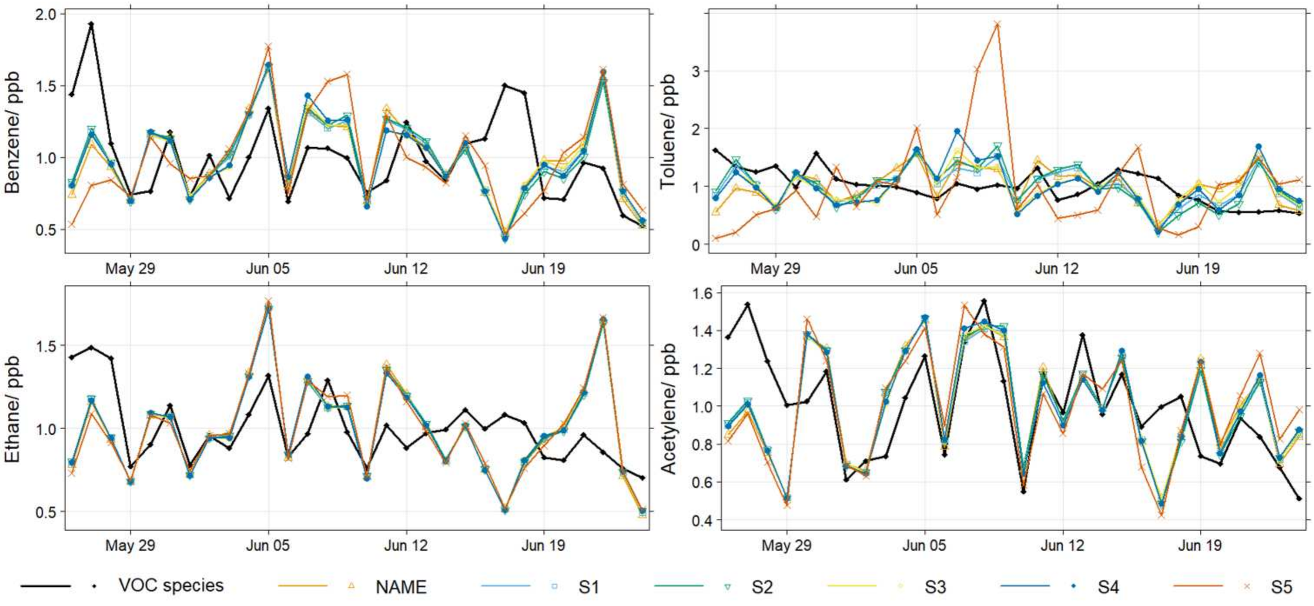

Figure 7: Normalised plots from the five modelled scenarios vs measured VOC concentrations during the summer campaign (scenarios are detailed in Table 1)

https://doi.org/10.5194/acp-2022-379
Preprint. Discussion started: 27 June 2022

Finally, the relationship between NO_x, VOCs and O_3 for the measurements and for the S1 base scenario was investigated to understand the differences in sources between winter and summer and to investigate whether the modelled VOCs follow the same relationship as the measured VOCs. In Figures 8 and 9, scatterplots of NO_x vs VOCs have been coloured by the mixing ratio of O_3 and are presented to investigate the difference between the winter and summer. It is important to understand how O_3 formation / production differs in the two seasons to accurately derive policies to tackle the O_3 pollution. During winter, the model follows the same relationship as the measured VOCs (Figure 8): O_3 is higher when NO_x and VOC levels are low. The relationship of the NO_x/VOC with O_3 during summer is slightly different compared to the winter (Figure 9). Moreover, it is observed that VOCs are highly correlated with the NO_x during the winter, indicating that NO_x and VOCs are possibly emitted from similar sources, however during the summer that relationship does not appear. During summer, the measurements suggest that O_3 is higher during low NO_x levels but shows no direct relationship with the VOCs concentrations. The results reveal the need for separate policy measures during the winter and summer. The other scenarios follow the same relationship as the base scenario S1 and the measurements.

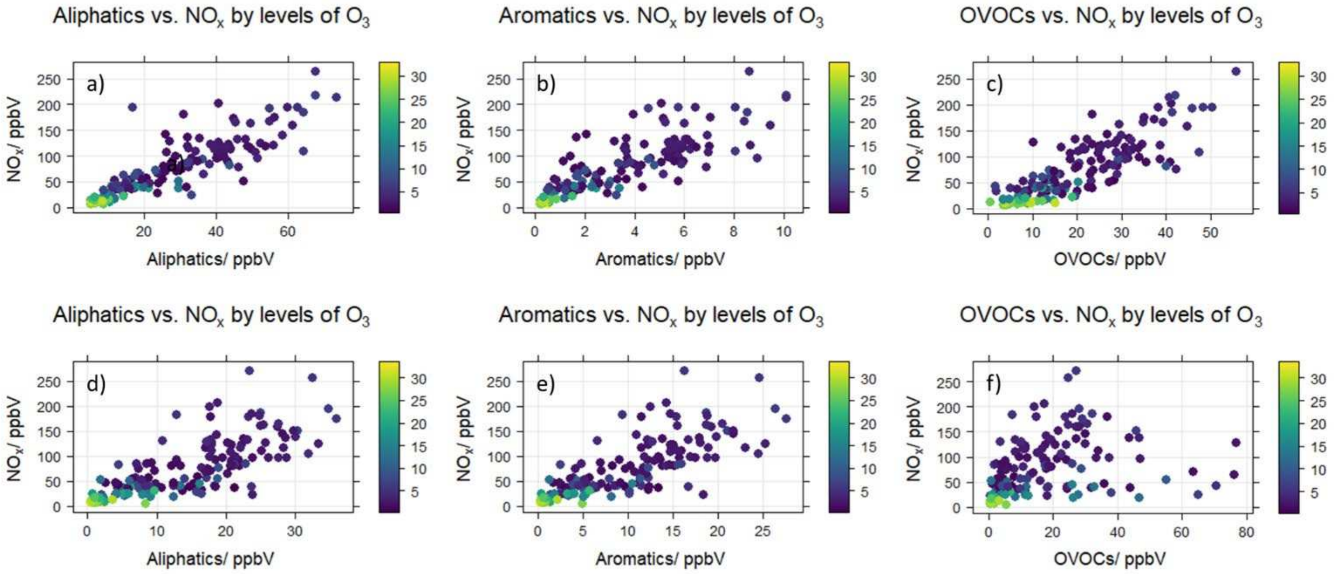

Figure 8: NO_x/VOC relationship with O_3 levels (colour bar in ppbV) during the winter campaign, (a-c): measured VOCs, (d-f): modelled VOCs (S1)

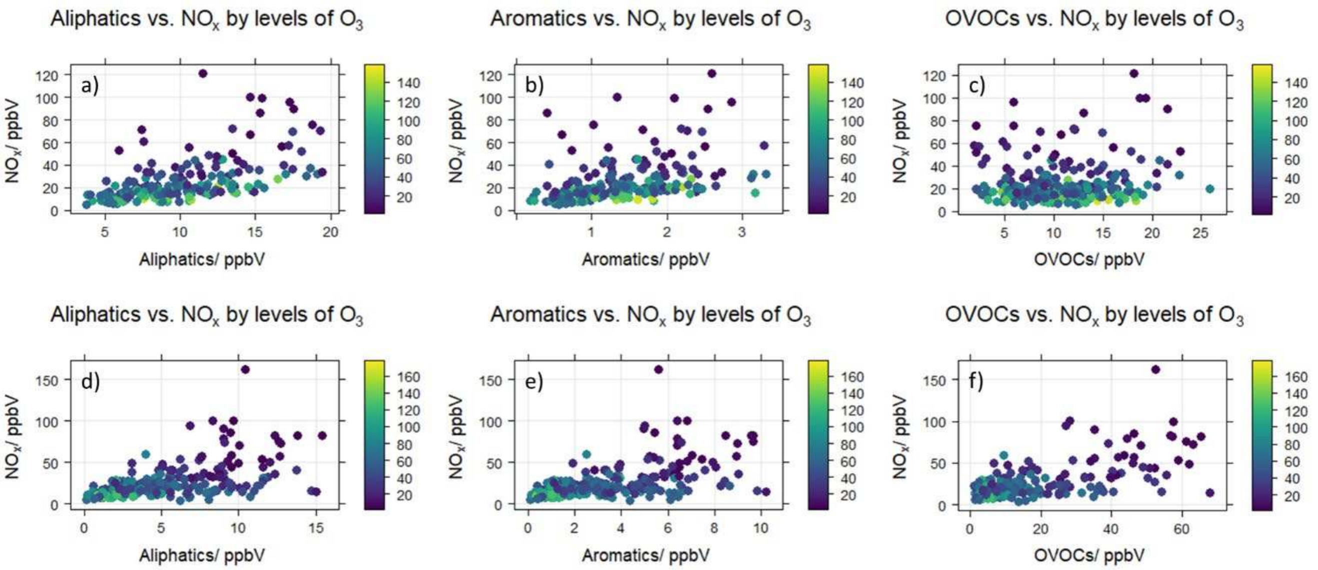

Figure 9: NOx/VOC relationship with O_3 levels (colour bar in ppbV) during the summer campaign, (a-c): measured VOCs, (d-f): modelled VOCs (S1)

3.4 OVOCs - Formaldehyde Production

As indicated by the model results (see Table 1), the formaldehyde concentration rapidly increases through photochemical reactions in the first 24 hours of transport, in addition to its direct emissions. Through photolysis, formaldehyde leads to new hydroxyl (OH) and hydroperoxy radicals (HO_2) which drive the O_3 production (Calvert et al., 2015). To understand how formaldehyde is produced in the air masses traveling to Beijing, additional runs of the AtChem2 box model were made with anthropogenic formaldehyde emissions set to zero for all scenarios. In these runs the model used a chemical mechanism containing only inorganic chemistry and methane, (set to a constant concentration of CH_4 1.989 ppm) with no other VOCs present. These tests show the amount of formaldehyde produced by the oxidation of CH_4 and allow for the calculation of the amount of formaldehyde produced from the reactions of the other VOCs with OH (by subtracting the anthropogenic formaldehyde measured with NAME and the formaldehyde produced by CH_4 from the total formaldehyde reported in each scenario), within 24 hours of travel from Beijing (Table 2).

Table 2: Average concentrations of formaldehyde produced via different processes in each model scenario (units in ppbV)

	CH_4 Oxidation	**NMVOCs Oxidation**	**Anthropogenic Emissions**	**CH_4 Oxidation**	**NMVOCs Oxidation**	**Anthropogenic Emissions**
	Winter Campaign			**Summer Campaign**		
S1[a]	0.04	7.07	0.76	0.92	10.95	0.43
S2[b]	0.09	9.31	0.76	1.42	11.49	0.43
S3[c]	0.09	15.09	0.76	1.33	10.48	0.43
S4[d]	0.17	17.71	0.76	1.85	10.32	0.43
S5[e]	2.15	24.43	0.76	2.06	8.47	0.43

[a]S1: Constraining original measurements (O_3, NO_2, NO, CO measured at the IAP tower) in NAME-AtChem2 runs
[b]S2: Constraining original measurements and doubling O_3 in NAME-AtChem2 runs
[c]S3: Constraining original measurements and halving NO_2 and NO in NAME-AtChem2 runs
[d]S4: Constraining original measurements and doubling O_3 and halving NO_2 and NO in NAME-AtChem2 runs
[e]S5: Constraining OH measurements only in NAME-AtChem2 runs

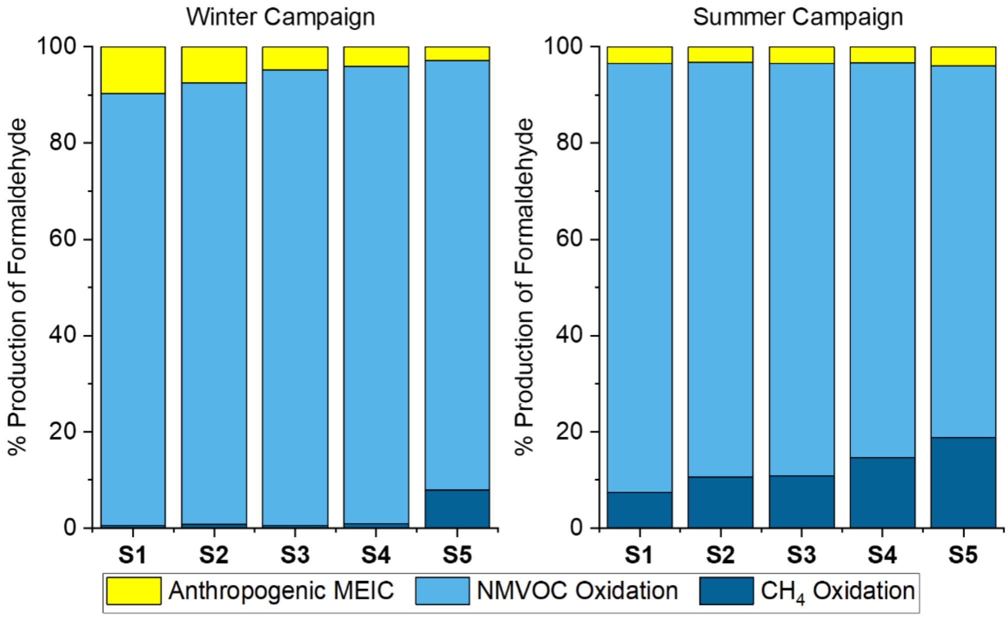

Figure 10: Relative production of formaldehyde via different processes during the summer and winter campaigns

Figure 10 presents the percentages of formaldehyde production in three categories during each scenario. The three categories are production via production by oxidation of CH_4, production by oxidation of other VOCs and production directly from anthropogenic sources. During both winter and summer the major source of formaldehyde is secondary formed formaldehyde produced by the oxidation of the rest of the VOCs investigated in this study. During the winter campaign, formaldehyde produced by CH_4 oxidation is less than 1% for all scenarios except S5 (approximately 8%). However, during the summer campaign an increase in the formaldehyde produced by CH_4 oxidation is observed from all scenarios. The highest production through CH_4 oxidation is observed with S5 with approximately 19% and the lowest in S1 with 7%.

3.5 Ozone Formation Potential

The production of O_3 can be limited either by the availability of VOCs or by the availability of NO_x and studies show that the O_3 increase in China is largely related to the increase in VOC emissions, with different species having different contribution to the O_3 formation (Cheng et al., 2010, Geng et al., 2009, Li et al., 2020). Therefore, to understand more about the effect of the VOCs on the formation of ozone, the ozone formation potential (OFP) was calculated using the concentrations of modelled and measured VOCs (in µg m^{-3}) and the Maximum Incremental Reactivity (MIR). The MIR is different for each species and represents the amount of ozone formed per gram of VOC (g O_3/g VOC) (Carter, 1994). The value of MIR indicates the individual contributions of each VOC to total ozone formation. The equation (eq. (1)) for calculating OFP is:

$$OFP_i = MIR_i \times VOC_i \tag{1}$$

Table 3: OFP from each scenario

Species	S1[a]	S2[b]	S3[c]	S4[d]	S5[e]
Winter					
Hydrocarbons	164	156	140	131	66
OVOCs	122	148	214	244	340
Total	286	304	354	375	406
Summer					
Hydrocarbons	47	34	38	26	21
OVOCs	155	165	153	157	138
Total	202	199	191	183	159

[a] S1: Constraining original measurements (O_3, NO_2, NO, CO measured at the IAP tower) in NAME-AtChem2 runs
[b] S2: Constraining original measurements and doubling O_3 in NAME-AtChem2 runs
[c] S3: Constraining original measurements and halving NO_2 and NO in NAME-AtChem2 runs
[d] S4: Constraining original measurements and doubling O_3 and halving NO_2 and NO in NAME-AtChem2 runs
[e] S5: Constraining OH measurements only in NAME-AtChem2 runs

It is observed that scenario S5 (OH measurements constrained) has the lowest overall ozone formation potential for VOCs, because the high OH decreases the concentrations of VOCs which decreases the formation of O_3 in a VOC limited environment (Table 3). As it was observed earlier, OVOCs have low anthropogenic emissions but are very rapidly produced in the atmosphere by photochemical reactions and then through photolysis they produce new hydroxyl (OH) and hydroperoxy radicals (HO_2) which in turn drive O_3 production. During the summer campaign, there is a lower ozone formation potential owing to the decreased concentrations of the VOCs. The OFPs for the VOCs indicate that during the winter period the OFP is higher due to the higher concentrations of the species than summer except for formaldehyde, which is higher during the summer. This is in agreement with the findings of Yang et al. (2018b), determined that during the summer of 2008 the OVOCs were the key species of the O_3 production.

3.6 Comparison of NAME-AtChem2 to GEOS-Chem

Table 4 compares the results of the runs with NAME-AtChem2 with daily 24-hour mean surface VOC concentrations from GEOS-Chem and the VOC measurements. The results shows that GEOS-Chem observed benzene and toluene concentrations by about 6 times larger for benzene and 6 – 15 (S1 – S5) times larger for toluene than the estimates from NAME-AtChem2. The high overestimations of aromatics in GEOS-Chem could possibly be due to underestimations in OH and in the oxidation rates of these VOCs (Miller et al., 2016). NAME-AtChem2 overestimates formaldehyde by 2 – 8 times (S1 – S5) and has a greater underestimate in ethanol than GEOS-Chem. Both GEOS-Chem and NAME-AtChem2 underestimate ethane by 1.7 times and approximately 2.5 times respectively. Owing to large differences between the modelled mean values from each model and consistency in day-to-day variability, the daily values were normalised by their mean (average concentration during study period for each species individually – November 2016) for visualisation purposes and compared to the measured VOCs to investigate whether the models agree with the observed patterns and sources affecting VOCs in Beijing (Figure 11). The greatest correlation between GEOS-Chem and NAME-AtChem2 daily means were for the S5 scenario with ethanol, benzene and propane showing the highest correlations of 0.67, 0.63 and 0.64, respectively.

As observed from the comparison of the modelled runs with the measured VOCs, both GEOS-Chem and NAME-AtChem2 methods can broadly capture the daily variation in the VOC concentrations from the use of monthly emission inventories. GEOS-Chem uses emission inventories to derive the NO_x and O_3 concentrations at each grid, while NAME-AtChem2 uses measured data from a single point and assumes concentrations are the same throughout the footprints, which can explain some of the discrepancies in the modelled concentrations between each method. Furthermore, the resolution of the GEOS-Chem simulations is coarser compared to the NAME-AtChem2 runs. Last but not least, the chemistry schemes used in the two models are different which can also result in some differences in the modelled concentrations.

Table 4: Average concentrations from NAME-AtChem2 scenarios, GEOS-Chem and measured VOCs during winter campaign (units in ppbV)

VOC	**Measured**[a]	**GEOS-Chem**[b]	**NAME**[c]	**S1**[d]	**S2**[e]	**S3**[f]	**S4**[g]	**S5**[h]
Benzene	1.5	12.4	2.1	2.1	2.0	2.0	2.0	1.7
Toluene	1.7	43.0	7.8	7.1	6.8	6.1	5.7	2.9
Ethane	8.6	5.0	3.4	3.4	3.4	3.4	3.4	3.2
Propane	6.0	11.2	3.7	3.6	3.6	3.5	3.4	3.0
Acetone	7.2	3.8	0.6	1.0	1.2	1.6	1.8	3.9
Formaldehyde	1.9	3.3	0.8	7.9	10.2	15.9	18.6	27.4
Ethanol	11.7	8.3	6.5	6.1	5.9	5.6	5.3	3.6

[a] Mean campaign average
[b] Modelled values from GEOS-Chem simulations
[c] Modelled values from the combination of MEIC and NAME
[d] S1: Constraining original measurements (O_3, NO_2, NO, CO measured at the IAP tower) in NAME-AtChem2 runs
[e] S2: Constraining original measurements and doubling O_3 in NAME-AtChem2 runs
[f] S3: Constraining original measurements and halving NO_2 and NO in NAME-AtChem2 runs
[g] S4: Constraining original measurements and doubling O_3 and halving NO_2 and NO in NAME-AtChem2 runs
[h] S5: Constraining OH measurements only in NAME-AtChem2 runs

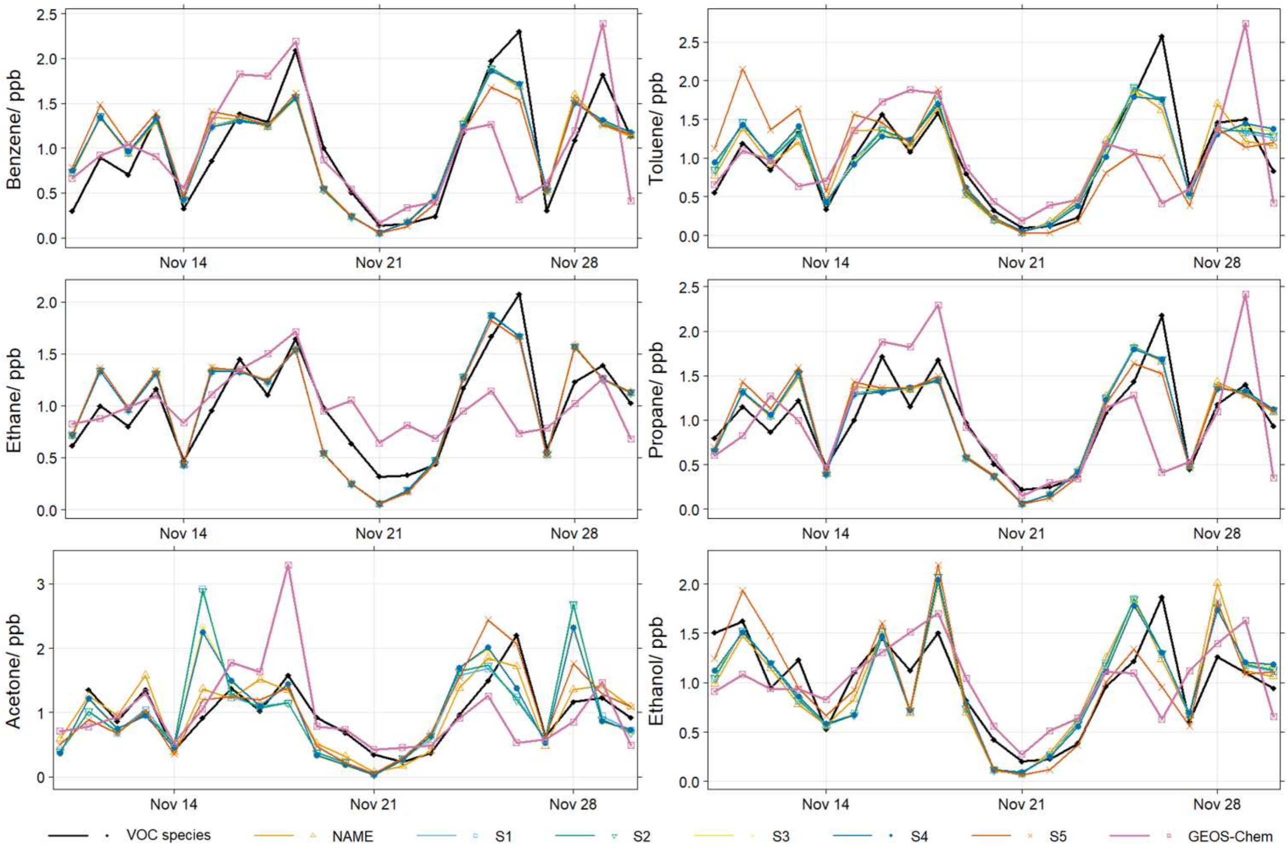

Figure 11: Comparison of day-to-day variability in observed and modelled VOCs. Normalised by mean (November 2016) time series of NAME without chemistry (NAME), NAME-AtChem2 (S1 – S5) vs GEOS-Chem vs measured VOC during the winter campaign

4 Conclusions

In this study, we investigated the capability to model VOCs concentrations in Beijing during the winter and summer APHH campaigns using a number of different approaches, and explored the effects that NO_x and O_3 levels have on VOC concentrations and the effect of the VOC concentrations on O_3 formation. Moreover, the production of formaldehyde was investigated during both campaigns.

Initially, modelled CO was used to calculate VOCs using the average measured VOC/CO ratio. The results indicate that one is able to reasonably predict the VOC concentrations by multiplying the measured ratio by CO. However, there are limitations to this method as a longer VOC dataset is needed to investigate the hypothesis and confirm that the relationship holds over longer time periods. This technique can be used for a rapid understanding of the VOC levels when VOC and CO measurements are not present by using just CO emission inventories and the NAME model with the measured VOC/CO of previous years.

Another approach is to combine the footprints calculated with the NAME model with the emission inventories and use the resulting VOC levels as inputs to inform the AtChem2 chemical box model, in order to account for chemical processing of air masses during transport into Beijing. During the winter period this method is able to capture the variations in the VOC concentrations well compared with the measurements. Moreover, the method is in good agreement with the GEOS-Chem chemical transport model. Comparing the last two methods, which have very different approaches and assumptions, reveals the importance of understanding how using different parameters in the modelling of chemical processes can affect the results and how this can subsequently affect policy making. In particular, the two methods show differences in the modelled concentrations of the species due to their different approaches, which could lead to different policy decisions being taken.

Through the combination of NAME, emission inventories and AtChem2 it was determined that during winter, the majority of the emissions affecting VOC levels in Beijing are from local sources and their concentrations are controlled by the chemistry in Beijing. However, during summer the transportation of pollutants from outside Beijing increases owing to the increase of the air mass transport from the industrial regions south of Beijing, which affects, along with the chemistry in those regions and within Beijing, the concentrations measured in Beijing. One of the limitations of coupling NAME with the AtChem2 box model, owing to the fact that it assumes homogeneous “pollution” along the whole transport pathway. This is not realistic in long-range transportation owing to varying atmospheric conditions and emission sources along the pathways. However, within one day of travel and when the majority of sources affecting during the two periods are local, then these scenarios can help understand how different atmospheric conditions can affect the VOC levels not only in Beijing but also in other regions around the world. The five scenarios suggest that OH levels dominate the chemistry of the species in both winter and summer, with higher OH revealing higher loss (for hydrocarbons) and production (for OVOCs) of the VOC species. Furthermore, higher OH will decrease transport from outside of Beijing since loss of the VOCs will take place faster before they arrive at Beijing.

The highest destruction observed with high OH was on ethene and toluene at approximately 63% and 75%, respectively. However, high OH in winter was also associated with the highest production of OVOCs, such as acetone and formaldehyde, which increased by approximately 550% and 3500% respectively within the first 24 hours after they were emitted, compared to the concentrations calculated with no chemistry. The highest production for formaldehyde, with an increase of 3000% during the summer, took place while O_3 was double the initial concentrations indicating that at higher O_3 levels, formaldehyde is also higher. The production of formaldehyde was further investigated in this study and it was determined that the majority of the formaldehyde is produced from the oxidation of NMVOCs in the atmosphere during both campaigns. However, increased production of formaldehyde from CH_4 is observed in the summer. With the highest in S5 at approximately 19% compared to the winter S5 at 8%.

The O_3 formation potential was calculated to determine that species such as formaldehyde, ethene and toluene are the highest contributors to ozone formation potential due to their higher maximum incremental reactivities; therefore at high concentrations of these three species the OFP increases. Reducing the concentrations of the VOCs investigated in this study will have a positive effect on reducing O_3 formation, but also on the formation of formaldehyde, which can itself increase ozone formation. For more effective control of VOCs and consequently O_3 in Beijing, the combination of NAME with emission inventories results suggest that the industrial sources need to be more effectively regulated during both seasons within and outside Beijing since they lead to the highest pollution events in Beijing. Moreover, the relationship between NO_x and VOCs reveal the possibility that different control measures need to be implemented during winter and summer, specifically focusing on both NO_x and VOC emissions during the winter, and more on the VOC emissions during the summer. Finally, more accurate emission inventories are needed to reduce uncertainties for deriving policy controls.

Data availability. Atmospheric measurement data used in this study are available from the CEDA data archive at https://catalogue.ceda.ac.uk/uuid/648246d2bdc7460b8159a8f9daee7844 (Fleming et al., 2017). Dispersion model footprints are available from CEDA at https: //catalogue.ceda.ac.uk/uuid/88f3a3de77354692aeada98c5dad599b (Panagi and Fleming, 2017). The modelled data in this study (modelled CO and air mass distribution) are available from the corresponding authors upon request.

Author contributions

MP performed the modelling and numerical data analysis, and led the manuscript development, RS contributed to the modelling analysis and data interpretation, ZF contributed to the development of the modelling and visualization technique, PSM contributed to research question framing and vision and the manuscript, EAM and GL performed the GEOS-Chem runs JH and AL collected the VOC APHH campaign data, ZQ contributed MEIC inventory data, JL and FS collected the NO, NO_2, O_3 and CO APHH campaign data, LW, ES, DH, RWM and CY collected the OH and HCHO APHH campaign data, JV oversaw the research and contributed extensively to the manuscript development and data interpretation. All co-authors contributed to the development of the manuscript.

Competing Interests

The authors declare that they have no conflict of interest.

Acknowledgments

We would like to thank the UK Met Office for supplying the Unified Model Meteorological data and the use of the NAME model and the CEDA for providing space on the JASMIN supercomputer to run the model. We thank the University of Leicester's High Performance Computing services for supplying the necessary computing power for plotting and storing the model output and Duncan Law-Green at the University of Leicester for developing the code to plot and interpret the NAME model output. Finally, we would like to thank the National Centre for Atmospheric Science (NCAS) and NERC for funding. GL thanks the PhD studentships funded by China Scholarship Council. J.D. Vande Hey acknowledges funding from the NIHR HPRU in Environmental Exposures and Health at the University of Leicester. ES and RWM would like to thank the NERC SPHERES DTP for their PHD studentships

Reference

Acton, W. J. F., Huang, Z., Davison, B., Drysdale, W. S., Fu, P., Hollaway, M., Langford, B., Lee, J., Liu, Y., Metzger, S., Mullinger, N., Nemitz, E., Reeves, C. E., Squires, F. A., Vaughan, A. R., Wang, X., Wang, Z., Wild, O., Zhang, Q., Zhang, Y., and Hewitt, C. N.: Surface–atmosphere fluxes of volatile organic compounds in Beijing, Atmos. Chem. Phys., 20, 15101–15125, https://doi.org/10.5194/acp-20-15101-2020, 2020.

Atkinson, R.: Atmospheric chemistry of VOCs and NOx, Atmospheric Environment, 34(12-14), 2063-2101, doi:10.1016/s1352-2310(99)00460-4, 2000.

Brown, A., Milton, S., Cullen, M., Golding, B., Mitchell, J. and Shelly, A.: Unified Modeling and Prediction of Weather and Climate: A 25-Year Journey, Bulletin of the American Meteorological Society, 93(12), 1865-1877, doi:10.1175/bams-d-12-00018.1, 2012.

Calvert, J. G.; Orlando, J. J.; Stockwell, W. R.; Wallington, T. J. The Mechanisms of Reactions Influencing Atmospheric Ozone; Oxford University Press: New York, 2015.

Carter, W.: Development of Ozone Reactivity Scales for Volatile Organic Compounds, Air & Waste, 44(7), 881-899, doi:10.1080/1073161x.1994.10467290, 1994.

Carter, W. and Seinfeld, J.: Winter ozone formation and VOC incremental reactivities in the Upper Green River Basin of Wyoming, Atmospheric Environment, 50, 255-266, doi:10.1016/j.atmosenv.2011.12.025, 2012.

Cheng H, Guo H, Wang X, et al. On the relationship between ozone and its precursors in the Pearl River Delta: application of an observation-based model (OBM) [published correction appears in Environ Sci Pollut Res Int. 2010 Sep;17(8):1491-2]. Environ Sci Pollut Res Int. 2010;17(3):547-560. doi:10.1007/s11356-009-0247-9, 2010.

Cryer, D. R.: Measurements of hydroxyl radical reactivity and formaldehyde in the atmosphere, PhD Thesis, University of Leeds, 2016

Donnelly, A., Naughton, O., Misstear, B. and Broderick, B.: Maximizing the spatial representativeness of NO2monitoring data using a combination of local wind-based sectoral division and seasonal and diurnal correction factors, Journal of Environmental Science and Health, Part A, 51(12), 1003-1011, doi:10.1080/10934529.2016.1198174, 2016.

Fleming, Z. L., Lee, J. D., Liu, D., Acton, J., Huang, Z., Wang, X., Hewitt, N., Crilley, L., Kramer, L., Slater, E., Whalley, L., Ye, C., and Ingham, T.: APHH: Atmospheric measurements and model results for the Atmospheric Pollution & Human Health in a Chinese Megacity, Centre for Environmental Data Analysis. http://catalogue.ceda.ac.uk/uuid/648246d2bdc7460b8159a8f9daee7844, 2017.

Geng, F., Cai, C., Tie, X. et al. Analysis of VOC emissions using PCA/APCS receptor model at city of Shanghai, China. J Atmos Chem 62, 229–247, https://doi.org/10.1007/s10874-010-9150-5, 2009.

Giglio, L.; Randerson, J. T.; Van Der Werf, G. R.: Analysis of Daily, Monthly, and Annual Burned Area Using the Fourth-Generation Global Fire Emissions Database (GFED4). J. Geophys. Res. Biogeosciences, 118 (1), 317–328. https://doi.org/10.1002/jgrg.20042, 2013.

Gu, Y., Li, Q., Wei, D., Gao, L., Tan, L., Su, G., Liu, G., Liu, W., Li, C. and Wang, Q.: Emission characteristics of 99 NMVOCs in different seasonal days and the relationship with air quality parameters in Beijing, China, Ecotoxicology and Environmental Safety, 169, 797-806, doi:10.1016/j.ecoenv.2018.11.091, 2019.

Guenther, A. B., Jiang, X., Heald, C. L., Sakulyanontvittaya, T., Duhl, T., Emmons, L. K., and Wang, X.: The Model of Emissions of Gases and Aerosols from Nature version 2.1 (MEGAN2.1): an extended and updated framework for modeling biogenic emissions, Geosci. Model Dev., 5, 1471–1492, https://doi.org/10.5194/gmd-5-1471-2012, 2012.

Hopkins, J. R., Jones, C. E., Lewis, A. C.: A dual channel gas chromatograph for atmospheric analysis of volatile organic compounds including oxygenated and monoterpene compounds, J. Environ. Monit., 13, 2268–2276., 2011.

Hoesly, R. M., Smith, S. J., Feng, L., Klimont, Z., Janssens-Maenhout, G., Pitkanen, T., Seibert, J. J., Vu, L., Andres, R. J., Bolt, R. M., Bond, T. C., Dawidowski, L., Kholod, N., Kurokawa, J.-I., Li, M., Liu, L., Lu, Z., Moura, M. C. P., O'Rourke, P. R., and Zhang, Q.: Historical (1750–2014) anthropogenic emissions of reactive gases and aerosols from the Community Emissions Data System (CEDS), Geosci. Model Dev., 11, 369–408, https://doi.org/10.5194/gmd-11-369-2018, 2018.

Hudman, R. C., Moore N. E., Martin R. V., Russell A. R., Mebust A. K., Valin L. C., and Cohen R. C.: A mechanistic model of global soil nitric oxide emissions: implementation and space based-constraints, Atm. Chem. Phys., **12**, 7779-7795, doi:10.5194/acp-12-7779-2012, 2012.

Jones, A., Thomson, D., Hort, M., Devenish, B.: The UK Met Office's next-generation atmospheric dispersion model, NAME III. Air Pollut. Model.Appl. XVII 17, 580–589, 2007

Karl, T., Striednig, M., Graus, M., Hammerle, A. and Wohlfahrt, G.: Urban flux measurements reveal a large pool of oxygenated volatile organic compound emissions, Proceedings of the National Academy of Sciences, 115(6), 1186-1191, doi:10.1073/pnas.1714715115, 2018.

LaFranchi, B. W., Goldstein, A. H., and Cohen, R. C.: Observations of the temperature dependent response of ozone to NOx reductions in the Sacramento, CA urban plume, Atmos. Chem. Phys., 11, 6945–6960, https://doi.org/10.5194/acp-11-6945-2011, 2011.

Li, J., Xie, S. D., Zeng, L. M., Li, L. Y., Li, Y. Q., and Wu, R. R.: Characterization of ambient volatile organic compounds and their sources in Beijing, before, during, and after Asia-Pacific Economic Cooperation China 2014, Atmos. Chem. Phys., 15, 7945–7959, https://doi.org/10.5194/acp-15-7945-2015, 2015.

Li, M., Zhang, Q., Kurokawa, J., Woo, J., He, K., Lu, Z., Ohara, T., Song, Y., Streets, D., Carmichael, G., Cheng, Y., Hong, C., Huo, H., Jiang, X., Kang, S., Liu, F., Su, H. and Zheng, B.: MIX: a mosaic Asian anthropogenic emission inventory under the international collaboration framework of the MICS-Asia and HTAP, Atmospheric Chemistry and Physics, 17(2), 935-963, doi:10.5194/acp-17-935-2017, 2017.

Li, K., Jacob, D., Liao, H., Shen, L., Zhang, Q. and Bates, K.: Anthropogenic drivers of 2013–2017 trends in summer surface ozone in China, Proceedings of the National Academy of Sciences, 116(2), 422-427, doi:10.1073/pnas.1812168116, 2019a.

Li, K., Jacob, D., Liao, H., Zhu, J., Shah, V., Shen, L., Bates, K., Zhang, Q. and Zhai, S.: A two-pollutant strategy for improving ozone and particulate air quality in China, Nature Geoscience, 12(11), 906-910, doi:10.1038/s41561-019-0464-x, 2019b.

Li, M., Zhang, Q., Zheng, B., Tong, D., Lei, Y., Liu, F., Hong, C., Kang, S., Yan, L., Zhang, Y., Bo, Y., Su, H., Cheng, Y., and He, K.: Persistent growth of anthropogenic non-methane volatile organic compound (NMVOC) emissions in China during 1990–2017: drivers, speciation and ozone formation potential, Atmos. Chem. Phys., 19, 8897–8913, https://doi.org/10.5194/acp-19-8897-2019, 2019c.

Li, Q. Q., Su, G. J., Li, C. Q., Liu, P. F., Zhao, X. X., Zhang, C. L., Sun, X., Mu, Y. J., Wu, M. G., Wang, Q. L. & Sun, B. H.: An investigation into the role of VOCs in SOA and ozone production in Beijing, China. Science of the Total Environment, 720, 2020.

Liu, J., Mauzerall, D. L., Chen, Q., Zhang, Q., Song, Y., Peng, W., Klimont, Z., Qiu, X. H., Zhang, S. Q., Hu, M., Lin, W. L., Smith, K. R., and Zhu, T.: Air pollutant emissions from Chinese households: A major and underappreciated ambient pollution source, P. Natl. Acad. Sci. USA, 113, 7756–7761, https://doi.org/10.1073/pnas.1604537113, 2016.

Liu, H., Liu, S., Xue, B., Lv, Z., Meng, Z., Yang, X., Xue, T., Yu, Q., and He, K.: Ground-level ozone pollution and its health impacts in China, Atmospheric Environment, 173, 223-230, https://doi.org/10.1016/j.atmosenv.2017.11.014, 2018.

Lu, G., Marais, E. A., Vu, T. V., Xu, J., Shi, Z., Lee, J. D., Zhang, Q., Shen, L., Luo, G., and Yu, F.: Assessment of strict autumn-winter emission controls on air quality in the Beijing-Tianjin-Hebei region, Atmos. Chem. Phys. Discuss. [preprint], https://doi.org/10.5194/acp-2021-428, 2021.

McDonald, B., de Gouw, J., Gilman, J., Jathar, S., Akherati, A., Cappa, C., Jimenez, J., Lee-Taylor, J., Hayes, P., McKeen, S., Cui, Y., Kim, S., Gentner, D., Isaacman-VanWertz, G., Goldstein, A., Harley, R., Frost, G., Roberts, J., Ryerson, T. and Trainer, M.: Volatile chemical products emerging as largest petrochemical source of urban organic emissions, Science, 359(6377), 760-764, doi:10.1126/science.aaq0524, 2018.

Miller, C., Jacob, D. J., Abad, G., and Chance, K.: Hotspot of glyoxal over the Pearl River delta seen from the OMI satellite instrument: implications for emissions of aromatic hydrocarbons, Atmos. Chem. Phys., 16, 4631-4639, 10.5194/acp-16-4631-2016, 2016.

Monks, P. S., Granier, C., Fuzzi, S., Stohl, A., Williams, M. L., Akimoto, H., Amann, M., Baklanov, A., Baltensperger, U., Bey, I., Blake, N., Blake, R. S., Carslaw, K., Cooper, O. R., Dentener, F., Fowler, D., Fragkou, E., Frost, G. J., Generoso, S., Ginoux, P., Grewe, V., Guenther, A., Hansson, H. C., Henne, S., Hjorth, J., Hofzumahaus, A., Huntrieser, H., Isaksen, I. S. A., Jenkin, M. E., Kaiser, J., Kanakidou, M., Klimont, Z., Kulmala, M., Laj, P., Lawrence, M. G., Lee, J. D., Liousse, C., Maione, M., McFiggans, G., Metzger, A., Mieville, A., Moussiopoulos, N., Orlando, J. J., O'Dowd, C. D., Palmer, P. I., Parrish, D. D., Petzold, A., Platt, U., Poschl, U., Prevot, A. S. H., Reeves, C. E., Reimann, S., Rudich, Y., Sellegri, K., Steinbrecher, R., Simpson, D., ten Brink, H., Theloke, J., van der Werf, G. R., Vautard, R., Vestreng, V., Vlachokostas, C., and von Glasow, R.: Atmospheric composition change - global and regional air quality, Atmos Environ, 43, 5268-5350, DOI 10.1016/j.atmosenv.2009.08.021, 2009.

Monks, P. S., Archibald, A. T., Colette, A., Cooper, O., Coyle, M., Derwent, R., Fowler, D., Granier, C., Law, K. S., Mills, G. E., Stevenson, D. S., Tarasova, O., Thouret, V., von Schneidemesser, E., Sommariva, R., Wild, O., and Williams, M. L.:

Tropospheric ozone and its precursors from the urban to the global scale from air quality to short-lived climate forcer, Atmos. Chem. Phys., 15, 8889-8973, 10.5194/acp-15-8889-2015, 2015.

Oram, D., Ashfold, M., Laube, J., Gooch, L., Humphrey, S., Sturges, W., Leedham-Elvidge, E., Forster, G., Harris, N., Mead, M., Abu Samah, A., Phang, S., Chang-Feng, O., Lin, N., Wang, J., Baker, A., Brenninkmeijer, C. and Sherry, D.: A growing threat to the ozone layer from short-lived anthropogenic chlorocarbons, Atmospheric Chemistry and Physics Discussions, 1-20, doi:10.5194/acp-2017-497, 2017.

Panagi, M., Fleming, Z. L., Monks, P. S., Ashfold, M. J., Wild, O., Hollaway, M., Zhang, Q., Squires, F. A., and Vande Hey, J. D.: Investigating the regional contributions to air pollution in Beijing: a dispersion modelling study using CO as a tracer, Atmos. Chem. Phys., 20, 2825–2838, https://doi.org/10.5194/acp-20-2825-2020, 2020.

Panagi, M. and Fleming, Z. L.: APHH: Atmospheric dispersion model footprint plots made at the IAP-Beijing site during the summer and winter campaigns, Centre for Environmental Data Analysis. https://catalogue.ceda.ac.uk/uuid/88f3a3de77354692aeada98c5dad599b, 2017.

Parrish, D., Kuster, W., Shao, M., Yokouchi, Y., Kondo, Y., Goldan, P., de Gouw, J., Koike, M. and Shirai, T.: Comparison of air pollutant emissions among mega-cities, Atmospheric Environment, 43(40), 6435-6441, doi:10.1016/j.atmosenv.2009.06.024, 2009.

Rumchev, K., Brown, H. and Spickett, J.: Volatile Organic Compounds: Do they present a risk to our health?, Reviews on Environmental Health, 22(1), doi:10.1515/reveh.2007.22.1.39, 2007.

Saikawa, E., Kim, H., Zhong, M., Avramov, A., Zhao, Y., Janssens-Maenhout, G., Kurokawa, J.-I., Klimont, Z., Wagner, F., Naik, V., Horowitz, L. W., and Zhang, Q.: Comparison of emissions inventories of anthropogenic air pollutants and greenhouse gases in China, Atmos. Chem. Phys., 17, 6393–6421, https://doi.org/10.5194/acp-17-6393-2017, 2017.

Sillman, S.: The relation between ozone, NOx and hydrocarbons in urban and polluted rural environments, Atmospheric Environment, 33(12), 1821-1845, doi:10.1016/s1352-2310(98)00345-8, 1999.

Shi, Z., Vu, T., Kotthaus, S., Harrison, R. M., Grimmond, S., Yue, S., Zhu, T., Lee, J., Han, Y., Demuzere, M., Dunmore, R. E., Ren, L., Liu, D., Wang, Y., Wild, O., Allan, J., Acton, W. J., Barlow, J., Barratt, B., Beddows, D., Bloss, W. J., Calzolai, G., Carruthers, D., Carslaw, D. C., Chan, Q., Chatzidiakou, L., Chen, Y., Crilley, L., Coe, H., Dai, T., Doherty, R., Duan, F., Fu, P., Ge, B., Ge, M., Guan, D., Hamilton, J. F., He, K., Heal, M., Heard, D., Hewitt, C. N., Hollaway, M., Hu, M., Ji, D., Jiang, X., Jones, R., Kalberer, M., Kelly, F. J., Kramer, L., Langford, B., Lin, C., Lewis, A. C., Li, J., Li, W., Liu, H., Liu, J., Loh, M., Lu, K., Lucarelli, F., Mann, G., McFiggans, G., Miller, M. R., Mills, G., Monk, P., Nemitz, E., O'Connor, F., Ouyang, B., Palmer, P. I., Percival, C., Popoola, O., Reeves, C., Rickard, A. R., Shao, L., Shi, G., Spracklen, D., Stevenson, D., Sun, Y., Sun, Z., Tao, S., Tong, S., Wang, Q., Wang, W., Wang, X., Wang, X., Wang, Z., Wei, L., Whalley, L., Wu, X., Wu, Z., Xie, P., Yang, F., Zhang, Q., Zhang, Y., Zhang, Y., and Zheng, M.: Introduction to the special issue "In-depth study of air pollution sources and processes within Beijing and its surrounding region (APHH-Beijing)", Atmos. Chem. Phys., 19, 7519–7546, https://doi.org/10.5194/acp-19-7519-2019, 2019.

Slater, E. J., Whalley, L. K., Woodward-Massey, R., Ye, C., Lee, J. D., Squires, F., Hopkins, J. R., Dunmore, R. E., Shaw, M., Hamilton, J. F., Lewis, A. C., Crilley, L. R., Kramer, L., Bloss, W., Vu, T., Sun, Y., Xu, W., Yue, S., Ren, L., Acton, W. J. F., Hewitt, C. N., Wang, X., Fu, P., and Heard, D. E.: Elevated levels of OH observed in haze events during wintertime in central Beijing, Atmos. Chem. Phys., 20, 14847–14871, https://doi.org/10.5194/acp-20-14847-2020, 2020.

Sommariva, R., Cox, S., Martin, C., Borońska, K., Young, J., Jimack, P., Pilling, M. J., Matthaios, V. N., Newland, M. J., Panagi, M., Bloss, W. J., Monks, P. S., and Rickard, A. R. (2019): AtChem, an open source box-model for the Master Chemical Mechanism, Geosci. Model Dev. Discuss., https://doi.org/10.5194/gmd-2019-192, 2020.

Tang, X., Bai, Y., Duong, A., Smith, M., Li, L. and Zhang, L.: Formaldehyde in China: Production, consumption, exposure levels, and health effects, Environment International, 35(8), 1210-1224, doi:10.1016/j.envint.2009.06.002, 2009.

Uysal, N., and Schapira, R. M.: Effects of ozone on lung function and lung diseases, Curr Opin Pulm Med, 9, 144-150, Doi 10.1097/00063198-200303000-00009, 2003.

von Schneidemesser, E., Monks, P. and Plass-Duelmer, C.: Global comparison of VOC and CO observations in urban areas, Atmospheric Environment, 44(39), 5053-5064, doi:10.1016/j.atmosenv.2010.09.010, 2010.

Wang, Y., Shen, L., Wu, S., Mickley, L., He, J. and Hao, J.: Sensitivity of surface ozone over China to 2000–2050 global changes of climate and emissions, Atmospheric Environment, 75, 374-382, doi:10.1016/j.atmosenv.2013.04.045, 2013.

Warneke, C., de Gouw, J., Holloway, J., Peischl, J., Ryerson, T., Atlas, E., Blake, D., Trainer, M. and Parrish, D.: Multiyear trends in volatile organic compounds in Los Angeles, California: Five decades of decreasing emissions, Journal of Geophysical Research: Atmospheres, 117(D21), n/a-n/a, doi:10.1029/2012jd017899, 2012.

Whalley, L. K., Slater, E. J., Woodward-Massey, R., Ye, C., Lee, J. D., Squires, F., Hopkins, J. R., Dunmore, R. E., Shaw, M., Hamilton, J. F., Lewis, A. C., Mehra, A., Worrall, S. D., Bacak, A., Bannan, T. J., Coe, H., Percival, C. J., Ouyang, B., Jones, R. L., Crilley, L. R., Kramer, L. J., Bloss, W. J., Vu, T., Kotthaus, S., Grimmond, S., Sun, Y., Xu, W., Yue, S., Ren, L., Acton, W. J. F., Hewitt, C. N., Wang, X., Fu, P., and Heard, D. E.: Evaluating the sensitivity of radical chemistry and ozone formation to ambient VOCs and NOx in Beijing, Atmos. Chem. Phys., 21, 2125–2147, https://doi.org/10.5194/acp-21-2125-2021, 2021.

Yang, W., Zhang, Y., Wang, X., Li, S., Zhu, M., Yu, Q., Li, G., Huang, Z., Zhang, H., Wu, Z., Song, W., Tan, J., and Shao, M.: Volatile organic compounds at a rural site in Beijing: influence of temporary emission control and wintertime heating, Atmos. Chem. Phys., 18, 12663–12682, https://doi.org/10.5194/acp-18-12663-2018, 2018a.

Yang, X., Xue, L., Wang, T., Wang, X., Gao, J., Lee, S., Blake, D. R., Chai, F., and Wang, W.: Observations and Explicit Modeling of Summertime Carbonyl Formation in Beijing: Identification of Key Precursor Species and Their Impact on Atmospheric Oxidation Chemistry, Journal of Geophysical Research (Atmospheres), 123, 1426-1440, 10.1002/2017jd027403, 2018b.

Yao, Z., Shen, X., Ye, Y., Cao, X., Jiang, X., Zhang, Y. and He, K.: On-road emission characteristics of VOCs from diesel trucks in Beijing, China, Atmospheric Environment, 103, 87-93, doi:10.1016/j.atmosenv.2014.12.028, 2015.

https://doi.org/10.5194/acp-2022-379
Preprint. Discussion started: 27 June 2022

Zhang, Z., Zhang, Y. L., Wang, X. M., Lu, S. J., Huang, Z. H., Huang, X. Y., Yang, W. Q., Wang, Y. S., and Zhang, Q.: Spatiotemporal patterns and source implications of aromatic hydrocarbons at six rural sites across China's developed coastal regions, J Geophys Res-Atmos, 121, 6669-6687, 10.1002/2016jd025115, 2016.

Zheng, B., Tong, D., Li, M., Liu, F., Hong, C. P., Geng, G. N., Li, H. Y., Li, X., Peng, L. Q., Qi, J., Yan, L., Zhang, Y. X., Zhao, H. Y., Zheng, Y. X., He, K. B. & Zhang, Q.: Trends in China's anthropogenic emissions since 2010 as the consequence of clean air actions. Atmospheric Chemistry and Physics, 18, 14095-14111, 2018.